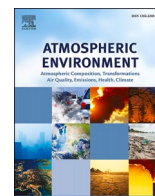




Contents lists available at ScienceDirect

# Atmospheric Environment

journal homepage: [www.elsevier.com/locate/atmosenv](http://www.elsevier.com/locate/atmosenv)

## Modeling expected air quality impacts of Oregon's proposed expanded clean fuels program

Yiting Li<sup>a</sup>, Guihua Wang<sup>b</sup>, Colin Murphy<sup>c</sup>, Michael J. Kleeman<sup>d,\*</sup><sup>a</sup> Department of Land, Air, and Water Resources, University of California, Davis, USA<sup>b</sup> Institute of Transportation Studies, University of California, Davis, USA<sup>c</sup> Policy Institute for Energy, Environment, and the Economy, University of California, Davis, USA<sup>d</sup> Department of Civil and Environmental Engineering, University of California, Davis, USA

### HIGHLIGHTS

- Air pollution impacts of low-carbon transportation fuel are evaluated in Oregon.
- Policies to reduce fuel carbon intensity reduce air pollution mortality.
- Annual public-health savings are equivalent to \$80M/yr.
- Exposure disparities based on race and income are reduced by 14–20%.
- Spatial distribution of each racial group determines air quality benefits.

### ARTICLE INFO

#### Keywords:

GHG reductions  
PM<sub>2.5</sub>  
PM<sub>0.1</sub>  
Environmental justice  
MOVES  
BenMAP

### ABSTRACT

The public health burden of traffic-related air pollution falls most heavily on the population living closest to major transportation corridors, which leads to exposure disparities between different socio-economic groups across the United States. The state of Oregon has adopted climate policies to reduce transportation fuel carbon intensity (CI). These climate policies have the potential co-benefit of reducing air pollution exposure disparities for different socio-economic groups. Here we analyze the emissions and air quality outcomes of three future year (2035) scenarios for transportation fuels in Oregon: (i) a Business as usual (BAU) scenario, (ii) a Clean Fuels Program (CFP) scenario that represents adoption and successful achievement of a proposed 25% reduction in carbon intensity in 2035; and (iii) a maximum ambition scenario (CFP MAX) that builds on the CFP scenario to achieve a 37% CI reduction by adopting low carbon fuels more aggressively, especially for heavy duty vehicles. Transportation emissions under all scenarios were estimated using the MOVES model for every county in Oregon. Detailed emissions with 4 km spatial resolution were then developed for each scenario by scaling the National Emissions Inventory (NEI) for the year 2017 based on the emissions derived from the MOVES analysis. Air quality in 2035 was simulated using the UCD/CIT chemical transport model that enables a detailed analysis of PM<sub>2.5</sub> and PM<sub>0.1</sub> components and sources. Exposure fields were analyzed using the BenMAP model to predict public health outcomes. Environmental justice analysis was conducted by race/ethnicity categories and income categories obtained from the American Community Survey (ACS). Results suggest that adoption of low-carbon transportation fuels will improve air quality in Oregon, yielding public health benefits equivalent to approximately \$80M/yr. Adoption of low carbon transportation fuels will also reduce disparities in exposure to transportation-related air pollution between residents in different race/ethnicity categories by ~14% in Portland and ~20% in Salem. Adoption of low-carbon fuels reduces PM<sub>2.5</sub> mass disparity by 10% in Salem, but does not have a significant effect in Portland, because on-road mobile sources contribute to less than 3% of the total PM<sub>2.5</sub> mass disparity in this city. The analysis reveals that the spatial distribution of each race/ethnicity group in each city is the primary factor that determines the impact of low carbon fuel adoption on exposure disparity.

\* Corresponding author.

E-mail address: [mjkleeman@ucdavis.edu](mailto:mjkleeman@ucdavis.edu) (M.J. Kleeman).

<https://doi.org/10.1016/j.atmosenv.2023.119582>

Received 15 July 2022; Received in revised form 12 December 2022; Accepted 2 January 2023

Available online 3 January 2023

1352-2310/© 2023 The Authors. Published by Elsevier Ltd. This is an open access article under the CC BY-NC-ND license (<http://creativecommons.org/licenses/by-nc-nd/4.0/>).

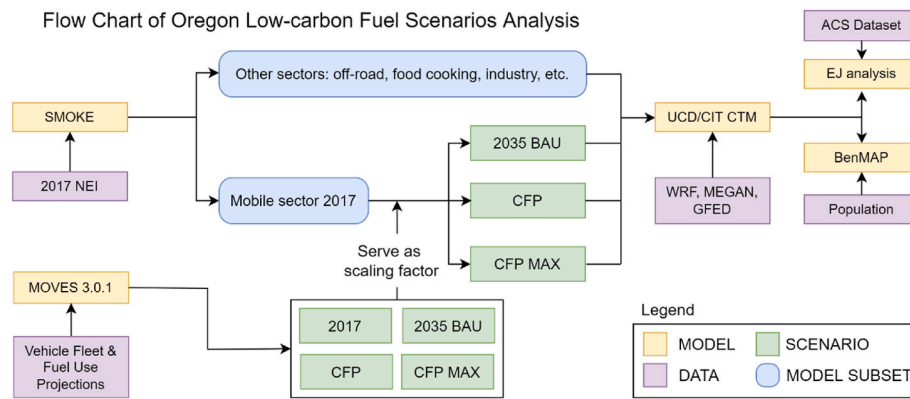


Fig. 1. Flow chart of Oregon Low-carbon Fuel Scenarios Analysis.

## 1. Introduction

Air pollution is associated with 7 million excess deaths across the globe each year, with 4.2 million of those losses attributed to outdoor air pollution (World Health Organization, 2021). Exposure to airborne particles with diameters less than  $2.5 \mu\text{m}$  ( $\text{PM}_{2.5}$ ) drives most of this air pollution mortality (Lelieveld et al., 2015). Toxicology studies show that ambient  $\text{PM}_{2.5}$  can be inhaled deep into the lungs, penetrate the gas-exchange region, and trigger inflammation. The smallest particles in the ultrafine size range with diameter less than  $0.1 \mu\text{m}$  ( $\text{PM}_{0.1}$ ) can pass through the respiratory barrier, and enter our circulatory system (Churg and Brauer, 2012; Pinkerton et al., 2000; Wang et al., 2013; Xing et al., 2016). Numerous epidemiological studies show that  $\text{PM}_{2.5}$  is closely associated with multiple adverse health effects in addition to premature death, including asthma, and cardiopulmonary diseases (Cohen et al., 2005; Goodkind et al., 2019; Krewski et al., 2009; Lepeule et al., 2012). Recent studies have found associations between health effects and  $\text{PM}_{2.5}$  mass at levels as low as  $5 \mu\text{g}/\text{m}^3$ , leading the World Health Organization (WHO) to lower their  $\text{PM}_{2.5}$  annual mean guideline value from  $10 \mu\text{g}/\text{m}^3$  to  $5 \mu\text{g}/\text{m}^3$  (World Health Organization, 2021).

Many environmental justice studies have documented the relationship between air pollution exposure, income, and race/ethnicity in the United States (Anderson et al., 2018; Banzhaf et al., 2019; Bell and Ebusu, 2012; Bravo et al., 2016; Colmer et al., 2020; Cushing et al., 2015; Liu et al., 2021; Miranda et al., 2011; Perlin et al., 2002; Tessum et al., 2021; Thakrar et al., 2020; Thind et al., 2019). Air pollution exposure disparities cause a public health burden for the groups with higher-exposure that inhibits their upward financial mobility and adds to the public health cost. The elimination of air pollution exposure disparities would better allow all people to reach their full potential in society.

The urgent need to address climate change offers a once-in-a-generation opportunity to redesign energy systems to simultaneously meet several objectives, including reduced emissions of Greenhouse Gases (GHGs), reduced emissions of air pollutants, and reduced levels of air pollution exposure disparity. Transportation emissions are a focal point for each of these objectives in the Western US, including California and Oregon, where residents rely on personal vehicles for mobility and heavy-duty vehicles for freight transport. The emissions from vehicles account for 30–40% of total GHG emissions (California Air Resource Board, 2021; Oregon, 2018) and the production and refining of petroleum-based transportation fuels is also a significant GHG source. There is a strong body of evidence (Wang et al., 2009) in the scientific literature confirming the net improvements in air quality associated with a transition from petroleum-fueled vehicles to non-petroleum alternatives (mainly caused by reduced tailpipe emissions) (Choma et al., 2021; Tessum et al., 2014).

California has adopted a suite of policies to reduce air pollutant and

GHG emissions from motor vehicles including tailpipe emission standards and Zero-Emission Vehicle (ZEV) requirements. Many of these policies have been adopted by other states, including Oregon. California launched the Low Carbon Fuel Standard (LCFS) in 2010 to encourage producers and importers of fuels to reduce their carbon intensity (CI) or procure lower-CI alternatives to meet the state's GHG emission target. Each of these climate mitigation regulations simultaneously reduced criteria pollutant and GHG emissions, leading to a reduction in environmental exposure disparity (see for example (Lewis et al., 2019; Li et al., 2022a,b; Sperling and Eggert, 2014; Winkler et al., 2018)).

The state of Oregon adopted its Clean Fuels Program (CFP) (based largely on California's LCFS) in 2010, though the program did not take effect until 2015. To date, Oregon's CFP has increased the share of non-petroleum fuels from approximately 7% to over 9% (Mazzone et al., 2021). In 2020, Governor Kate Brown issued Executive Order 20-04, which instructed state agencies to adopt a number of policies designed to further reduce the state's GHG emissions. Among them was an extension of Oregon's CFP with targets of at least 20% CI reduction in 2030 and 25% in 2035. To achieve this goal, the Oregon Department of Environmental Quality (DEQ) proposed several future low-carbon fuel scenarios that have the potential to reduce GHG emissions and improve air quality.

Here, we quantify the benefits to air quality and the reduction in exposure disparities associated with Oregon's clean transportation fuel program. Three future year 2035 scenarios are evaluated: a reference business as usual (BAU) scenario that accounts for current transportation-related regulations and trends, a CFP scenario (abbreviated as CFP) that corresponds to the proposed 25% reduction in transportation carbon intensity (CI) described by the Oregon CFP program, and a CFP MAX scenario (abbreviated as CFP MAX), which reduces transportation CI by 37% by replacing petroleum with renewable diesel for medium-/heavy-duty vehicles. CFP and CFP MAX scenarios were developed by the Oregon DEQ (ICF, 2021). Emissions with a 4 km spatial resolution are developed for each scenario and a regional chemical transport model (CTM) is used to predict air pollution exposure fields. Public health benefits associated with reduced transportation-related emissions in each scenario are calculated using standard epidemiological relationships provided by the EPA's Environmental Benefits Mapping and Analysis Program – Community Edition (BenMAP) program (Sacks et al., 2018). Air pollution exposures in the year 2035 are calculated for five household income groups and four household race/ethnicity groups defined by the American Community Survey (ACS). Environmental inequities are estimated for each socio-economic group in each emissions scenario. The reduction in air pollution exposure disparity under each GHG mitigation scenario is then discussed. The results of this study serve as a guide for other countries/states/regions that may wish to use similar CI-based fuel policies for GHG emissions reductions.

## 2. Methodology

On-road criteria pollutant emissions for the 2017 basecase, the 2035 BAU, the 2035 CFP, and the 2035 CFP MAX scenarios were developed using the EPA's Motor Vehicle Emission Simulator (MOVES) model (US EPA, 2021). The on-road emissions predicted by MOVES reflect expected reductions from the replacement of existing fuels with low-carbon alternatives. The post-emissions behavior of atmospheric pollutants and the resultant exposure fields were predicted using the UCD/CIT regional chemical transport model (CTM) (Kleeman et al., 1997; Venecek et al., 2019; Ying et al., 2007; Yu et al., 2019). The public health benefits of reduced CI were predicted using BenMAP-CE. Finally, an Environmental Justice (EJ) analysis was conducted based on air pollution exposure and household race/household income categories described by the American Community Survey (ACS) (United States Census Bureau, 2020). Fig. 1 illustrates the flow of data across the entire study, with further details presented in the following sections.

### 2.1. Developing the on-road emission inventory using MOVES

County-level emissions including criteria air pollutants for the 2017 basecase, 2035 BAU, 2035 CFP and 2035 CFP MAX scenarios were generated with MOVES 3.0.1 (US EPA, 2021). To better quantify Oregon's transportation emissions in the future, the MOVES model was calibrated by incorporating Oregon-specific activity forecast data, such as vehicle miles traveled (VMT) and vehicle population, rather than relying on the MOVES default data (see Tables S1 and S2). The calibrated MOVES output is hereafter referred to as the 2035 BAU scenario, which serves as the reference for comparisons with CFP and CFP MAX scenarios.

The emission impacts of CFP and CFP MAX were developed using modified VISION scenario tools (ICF, 2021) in which vehicle population, VMT, and fuel consumption are connected by the annual VMT accrual rates and fuel economy. Policy changes were reflected in the market share of alternative fuel vehicles including zero-emission vehicles (ZEVs). On-road mobile emissions from the 2035 BAU scenario were adjusted to represent the CFP and CFP MAX scenarios based on the difference in the market share of new sales of alternative fuel vehicles relative to the BAU scenario (see Tables S3–S7). A summary of statewide on-road emissions under each scenario is shown in Table S8.

The CFP scenario represents the expected changes in Oregon's vehicle fleet due to the adoption of California's Advanced Clean Trucks regulation, as well as the forthcoming Advanced Clean Cars 2 regulation, which will require rapid increases in ZEVs (primarily battery-electric vehicles) sales shares, resulting in the replacement of a significant fraction of Oregon's on-road transportation fleet with ZEVs by 2035 (ICF, 2021). These changes are sufficient to meet the 25% CI reduction target specified in the executive order.

The CFP MAX scenario evaluates additional policy-driven changes to Oregon's transportation system, in addition to those modeled in CFP. The primary difference between the two is the displacement of an additional quarter of the diesel demand by renewable diesel; CFP MAX also projects more compressed natural gas (CNG), electric, and hydrogen heavy-duty vehicles (class 7 & 8 trucks) than CFP. The composition of renewable diesel differs from its petroleum equivalent, most notably due to very low sulfur and reduced aromatic content. These changes in diesel fuel composition can reduce particulate matter (PM) emissions (see for

example Christopher Stoops, 2021; C.J.S. Bartlett et al., 1992; Qian et al., 2017) in vehicles that lack a diesel particulate filter (DPF). Most heavy duty diesel vehicles in the future Oregon fleet will be equipped with DPFs, minimizing the difference in expected PM emission rates between vehicles fueled by renewable diesel and those fueled by conventional diesel. The CFP MAX scenario slightly reduces emissions for most of the criteria pollutants relative to the CFP scenario, but the CFP MAX may emit slightly more CO and total hydrocarbons (THC) due to the addition of more heavy duty CNG trucks in this scenario. Total NOx emissions are not predicted to increase in the CFP MAX scenario under the assumption that the new CNG engines will use low-NOx technologies (Mahla et al., 2018; Zhu et al., 2020). In the 2035 timeframe, the overall emission impact of CNG and fuel cells is expected to be quite small because those heavy-duty vehicles only account for a small portion of the heavy-duty fleet compared to the larger number of light duty vehicles. In the longer term beyond the year 2035, fuel cells may play an important role in mitigating the emissions of criteria pollutants (and greenhouse gases) due to their cumulative vehicle stock growth in Oregon (ICF, 2021).

### 2.2. Current and future year emissions inventories

Current year (2017) basecase emissions inventories with 4 km spatial resolution were created from the EPA 2017 National Emissions Inventory (NEI) using the Sparse Matrix Operator Kernel Emissions (SMOKE-4.7) modeling system (US EPA, 2020). Emissions from all sectors were incorporated into the simulations, including mobile sources, commercial & residential sources, industrial sources, aircraft, and area sources, such as food cooking, etc. Wildfire emissions for historical years were estimated from the Global Fire Emissions Database (GFED) (Giglio et al., 2013; Werf et al., 2017). Biogenic emissions were generated using the Model of Emissions of Gases and Aerosols from Natural (MEGAN) (Guenther et al., 2012). The 2017 basecase emissions inventory was used to simulate a full year of pollutant concentrations for comparison to measured values as a quality control check before future simulations were performed.

Mobile emissions with 4 km spatial resolution were scaled for each county in Oregon at the Source Classification Code (SCC) level from the base year 2017 to the future year 2035, based on MOVES results using Eq. (1):

$$(NEI\ Mobile\ Emissions)_{SCC}^{2035} = (NEI\ Mobile\ Emissions)_{SCC}^{2017} \times \frac{(MOVES)_{SCC}^{2035}}{(MOVES)_{SCC}^{2017}} \quad (1)$$

Future year 2035 emissions from sectors other than mobile sources were maintained at their year 2017 basecase levels. This approach directly analyzes the effects of the transportation-oriented policies assuming that the chemical regime will remain unchanged between the years 2017 and 2035.

Table 1 summarizes the Oregon statewide emissions of oxides of nitrogen (NOx), airborne particulate matter (PM), oxides of sulfur (SOx), and ammonia (NH3) under the 2017 basecase, 2035BAU, 2035 CFP, and 2035 CFP MAX scenarios. Note that totals in Table 1 reflect emissions from mobile, point, and area sources so that the changes from the different mobile source scenarios can be understood in the context of the full emissions inventory. On-road gasoline tailpipe emissions account for 9% of NOx emissions, and 3% of PM<sub>2.5</sub> emissions across the state. On-road diesel tailpipe emissions account for 6% of NOx emissions and

**Table 1**

Air Pollution emissions summaries for Oregon under the 2017 basecase, 2035BAU, 2035CFP, and 2035CFP MAX scenarios.

	NOx (kmol/day)	PM (kg/day)	PM2.5 (kg/day)	SOX (kmol/day)	NH3 (kmol/day)
2017 basecase	55,141	462,542	247,468	5,793	5,948
2035 BAU	53,499	459,907	244,982	5,792	5,924
2035 CFP	52,594	458,182	243,279	5,790	5,890
2035 CFP MAX	52,570	458,167	243,266	5,790	5,889

2% of PM<sub>2.5</sub> emissions across the state. Emissions from on-road gasoline plus on-road diesel tailpipes could be as high as 20% of the NO<sub>x</sub> and PM<sub>2.5</sub> emissions totals in urban areas. Controls on non-transportation sources in Oregon were not explored in the current study, but results for California are discussed by Li et al. (2022a).

PM and NO<sub>x</sub> emissions strongly affect ambient PM<sub>2.5</sub> concentrations. Comparing the 2035 BAU and 2035 CFP scenarios, emissions from on-road gasoline vehicles are reduced by 25% for PM and 22% for NO<sub>x</sub>; emissions from on-road diesel vehicles are reduced by 2% for PM and 6% for NO<sub>x</sub>. Reductions from the 2035 CFP scenario to the 2035 CFP MAX scenario are modest, with only a 2% PM decrease and 2.13% NO<sub>x</sub> decrease for on-road diesel vehicles. The CFP MAX scenario replaces approximately one-quarter of conventional diesel fuel in the CFP scenario with renewable diesel and other reduced CI fuels in heavy-duty vehicles. All heavy-duty engines are assumed to have modern (post-2010 model year) emissions control systems that emit criteria pollutants at similar levels for conventional diesel and biodiesel fuel (Durbin et al., 2021).

## 2.3. Air quality simulation

### 2.3.1. Meteorology model

Hourly meteorology inputs to drive the regional chemical transport model at 4-km resolution during the years 2016 and 2030–2039 were simulated using the Weather Research and Forecasting (WRF) v4.3 model ([www.wrf-model.org](http://www.wrf-model.org)). The WRF model was configured with 31 vertical layers from the ground level to the top of the domain defined by an atmospheric pressure of 100 hPa. Initial and boundary conditions for meteorological simulations for the year 2016 were obtained from the North American Regional Reanalysis (NARR) database created by the National Center for Environmental Prediction (NCEP). Initial and boundary conditions for the year 2035 were obtained from the Community Climate System Model (CCSM) using the Representative Concentration Pathway (RCP) 4.5 Scenario (Gent et al., 2011).

### 2.3.2. Chemical transport model

The UCD/CIT airshed model is a reactive 3-D chemical transport model (CTM) that predicts the evolution of gas and particle phase pollutants in the atmosphere in the presence of emissions, transport, deposition, chemical reaction, and phase change (Kleeman et al., 1997; Ying et al., 2007). The basic capabilities of the UCD/CIT model are similar to the CMAQ model maintained by the US EPA, but the UCD/CIT model has additional source apportionments features and higher particle size resolution (Hu et al., 2014, 2015, 2017; Li et al., 2022a; Yu et al., 2019).

Source apportionment calculations for primary PM within the UCD/CIT model are accomplished using “tagging”. Emissions in the current study were tagged in nine separate sectors: 1) type 1 – onroad gasoline mobile; 2) type 2 – offroad gasoline equipment; 3) type 3 – onroad diesel mobile; 4) type 4 – offroad diesel equipment; 5) type 5 – wood burning; 6) type 6 – food cooking; 7) type 7 – aircraft; 8) type 8 – natural gas and biogenic; 9) type 9 – tire & brake wear and miscellaneous emissions not included in the categories listed above. An artificial tracer is emitted proportionally to emissions from each source category. Artificial tracers do not influence the particle radius and the dry deposition rates. Tracers are carried through all emissions, transport, deposition, coagulation, and growth calculations within the CTM framework so that they are directly proportional to the mass of primary particulate matter from each tracked source sector.

The low-carbon transportation fuel scenarios investigated in the current study will change the emissions of primary PM grouped within emissions sectors 1 (on-road gasoline) and 3 (on-road diesel) in the current UCD/CIT configuration. EVs use of regenerative braking typically reduces brake dust wear compared to conventional vehicles, however the magnitude of these effects are generally smaller than that of tailpipe ones, and were not modeled in this study. Mobile mitigation

strategies will also change the emissions of NO<sub>x</sub> and VOC that will affect the formation of secondary particulate matter components such as nitrate. These secondary effects are not “tagged”, but they can be calculated as the difference between PM concentrations under different emissions scenarios.

### 2.3.3. Long-term simulation strategy

The El Niño Southern Oscillation (ENSO) strongly affects meteorology and air quality in the Western US. ENSO cycles typically last seven years, making it necessary to simulate multi-year time periods (up to a decade long) in order to predict representative annual-average concentrations in future time periods. A more efficient strategy for long-term simulations samples a subset of simulation periods across a suitably long time window. The “sample” of predicted concentrations generated by this subset of simulation periods represents an unbiased estimate for the long-term concentrations, with the uncertainty of the estimate reduced as the number of sample points increases. For the present study, the long-term PM<sub>2.5</sub> and O<sub>3</sub> concentrations were calculated using eight randomly-selected episodes in each of the four seasons across the 10 year time window between 2030 and 2039. Each simulation episode had a duration of 7-days. Sensitivity analysis indicates that the average air pollution concentrations predicted over this thirty-two week sample captures the long-term average concentrations in California with a standard error of 0.23 μg/m<sup>3</sup> in the presence of the El Niño Southern Oscillation (ENSO) (Li et al., 2022a). The 32-week average concentrations constructed using this method are used as the long-term average concentration in Oregon for the time period centered on the year 2035.

## 2.4. BenMAP health impact analysis

The public health impacts of air pollution within each energy scenario were calculated using the BenMap-CE v1.4.8 model developed by US EPA (Sacks et al., 2018). The population dataset was prepared using PopGrid v4.3 (Census, 2010) according to the instructions provided in the BenMAP manual for the year 2010. Spatial patterns of income distribution and race/ethnicity in historical years were assumed to be strong predictors for those same features in future years.

BenMAP calculates differential health impacts between an exposure scenario and a reference case. The reference base in this study is the atmosphere without any anthropogenic pollutants (primary or secondary PM<sub>2.5</sub> from anthropogenic sources). The background concentration of total PM<sub>2.5</sub> mass is estimated to be 3 μg/m<sup>3</sup> in the western US, which is the concentration of marine aerosol measured near the Pacific Ocean. There is no natural background concentration for motor vehicle tailpipe emissions, and so the background concentration is set to 0 μg/m<sup>3</sup> during calculations for the health effects associated with these particles. Two sets of health impact comparisons were made in the current study. The 2035 BAU analysis uses the UCD/CIT year 2035 BAU simulation results as the high exposure scenario and a uniform PM<sub>2.5</sub> mass concentration of 3 μg/m<sup>3</sup> for the reference case. The effects of PM<sub>2.5</sub> emitted directly from the tailpipes of motor vehicles in the 2035 BAU are evaluated using the nominal PM<sub>2.5</sub> tracer mass as the high exposure scenario and 0 μg/m<sup>3</sup> for the reference case. The 2035 clean fuel analysis in future years uses the BAU scenario as the high exposure scenario and CFP or CFP MAX as the reference case. Health damages were estimated using results from (Krewski et al., 2009). Economic benefits were then calculated using the value of a statistical life (VSL) of \$7.6M (World Bank, 2016). Results are shown in Section 3.2.3.

## 2.5. Environmental justice analysis

Environmental justice analysis was conducted in two domains, shown in Fig. S1: Portland, the largest city in Oregon, and Salem, the capital city of Oregon. Socio-economic data from the American Community Survey (ACS) 2015–2016 (United States Census Bureau, 2020)

**Table 2**  
Household race/ethnicity Category summary in target analysis domain.

Race/Ethnicity	Salem		Portland	
	Household	Percentage	Household	Percentage
Total	99,384		556,152	
Hispanic	12,249	12.32%	46,793	8.41%
Black	813	0.82%	17,525	3.15%
non-Hispanic White	81,497	82.00%	438,497	78.84%
Asian	1,776	1.79%	34,115	6.13%

**Table 3**  
Household income category summary in target analysis domain.

Income Category	Salem		Portland	
	Household	Percentage	Household	Percentage
Total	99,384		556,152	
< \$24,999	20,818	20.95%	98,357	17.69%
\$25,000 – \$44,999	21,501	21.63%	96,379	17.33%
\$45,000 – \$99,999	38,099	38.24%	200,158	35.99%
> \$ 100,000	19,151	19.18%	161,258	29.00%

was used to calculate air pollution exposure for different household income and household race/ethnicity groups in Oregon.

Four categories of household race/ethnicity were analyzed: non-Hispanic White, Black and African American, Asian, and Hispanic or Latino, regardless of race. Non-Hispanic White residents account for ~80% of the population in both study cities (race/ethnicity summary shown in Table 2). The household race/ethnicity population densities are shown in Figs. S2–S5. Non-Hispanic White residents are distributed approximately uniformly across the cities of Portland and Salem (Fig. S5), but minorities primarily live in a subset of each city. Hispanic or Latino residents account for 12% of the population in Salem and 8% of the population in Portland. Asian and Black and African American residents account for less than 7% of total population in both Portland and Salem. Black and African American residents tend to live northeast of Portland (Fig. S3), while Asian (Fig. S2) and Hispanic or Latino (Fig. S4) residents live in Hillsboro (west of Portland) and east of Portland. Black and Hispanic or Latino residents live northwest of Salem close to the I-5 corridor (Figs. S3–4), but it is noteworthy that the total

population of black residents is much smaller than Hispanic residents (Fig. S3). Asian residents tend to live outside of urban core of both Portland and Salem (Fig. S2).

The ACS dataset includes 16 household income categories (shown in Table S9) at the census block level that were aggregated into 4 income categories in the present analysis in order to obtain sufficient statistical power within each category. Each of the combined income categories was created by combining the results from four of the original 16 income categories. Table 3 displays the definitions for each aggregated income category and the number of residents falling into each income category. The population densities for each aggregated income category are shown in Figs. S6–S9. For Portland, household incomes increase from the southwest portion of the city towards the northeast portion of the city. It is noteworthy that many Portland residents in the highest income category live in the downtown city core (home sales prices are also highest) where pollutant concentrations are generally higher (Fig. S9). There are no significant spatial patterns for the first three household income groups in Salem, but residents in the highest household income group tend to live outside of the urban core and away from major highways.

Oregon’s population is projected to grow by approximately 20% (~4M–5M) between 2017 and 2035. Scenarios describing regions that will grow most quickly and the economic/ethnic makeup of those new residents is beyond the scope of the current analysis. The relative demographic distributions were therefore assumed to remain constant between 2017 and 2035. Household Population weighted concentrations (HPWCs) were calculated for PM<sub>2.5</sub>, PM<sub>0.1</sub> and other species/tracers for each income category and for each race/ethnicity group under the three future transportation energy scenarios in Oregon. Absolute/relative exposure and absolute disparity were analyzed to determine the ability of each scenario to reduce air pollutant exposure for all residents and to mitigate the exposure disparity between income categories and races/ethnicity groups.

### 3. Results

#### 3.1. Chemical transport model output and quality control

Quality control simulations for the year 2016 were carried out across Oregon to build confidence in the inputs used to drive the source-

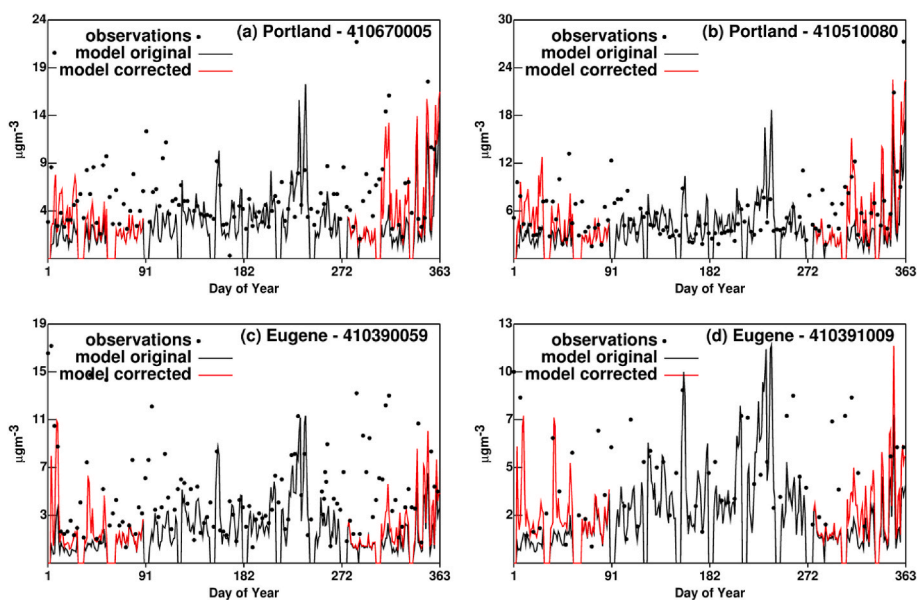


**Fig. 2.** Predicted and measured PM<sub>2.5</sub> mass concentrations in the year 2016. “Corrected” model results increased per-capita wood smoke emissions rates to be consistent with California emissions projections.

**Table 4**

Normalized Mean Bias (NMB), Normalized Mean Error (NME), and correlation coefficient between model predictions and measurements in the year 2016. Simulations meet target model performance criteria at three out of four measurement sites when corrections are applied to residential wood burning emissions.

	Original			Residential wood burning corrected		
	<0.3	< ±0.1	>0.79	<0.3	< ±0.1	>0.79
Goal*	<0.3	< ±0.1	>0.79	<0.3	< ±0.1	>0.79
Criteria*	<0.5	< ±0.3	>0.40	<0.5	< ±0.3	>0.40
Site	NMB	NME	r	NMB	NME	r
Portland - 410510080	0.44	-0.25	0.44	0.4	-0.07	0.67
Portland - 410670005	0.473	-0.4	0.33	0.37	-0.28	0.56
Eugene - 410390059	0.53	-0.5	0.15	0.47	-0.43	0.41
Eugene - 410391009	0.413	-0.35	0.45	0.37	-0.26	0.53

oriented UCD/CIT regional air quality model before it was applied to the year 2035 BAU, 2035 CFP, and 2035 CFP MAX simulations. Weak La Nina conditions prevailed in 2016, with slightly higher-than-average rainfall during winter months. Tests in 2016 should therefore be representative of typical ENSO conditions expected in future years. Meteorological data for 2016 had already been acquired as part of previous studies in California (Li et al., 2021; Li et al., 2022a). The EPA NEI inventories for 2017 were utilized for these simulations, as this was the closest available emissions inventories to the year 2016.

Predicted ambient annual average concentrations of PM<sub>2.5</sub> mass, element carbon (EC), organic carbon (OC), nitrate and PM<sub>0.1</sub> mass for the year 2016 are shown in Figs. S10–S11. Predicted ambient concentrations for primary PM<sub>2.5</sub> mass associated with tailpipe emissions from on-road gasoline vehicles and on-road diesel vehicles are shown in Fig. S12. The ambient concentrations associated with on-road vehicles are calculated using the tagging procedures discussed in Section 2.3.2. Concentrations of PM<sub>2.5</sub> mass and PM<sub>2.5</sub> components over land are highest in major cities such as Portland, Eugene and areas along the I-5 corridor in the year 2016. The PM<sub>2.5</sub> EC concentrations are primarily from on-road heavy duty diesel vehicles. The spatial pattern of EC is consistent with the spatial pattern of primary PM<sub>2.5</sub> mass emitted from the tailpipes of gasoline and diesel vehicles (Fig. S12). PM<sub>2.5</sub> OC concentrations are mainly from food cooking and residential wood combustion, with a spatial pattern that follows population density rather than major transportation corridors (Fig. S13).

Predicted PM<sub>2.5</sub> mass concentrations were compared to measurements in urban areas, including Portland (Fig. 2a and b), and Eugene (Fig. 2c and d). Fig. S14 shows the map of available measurement sites in Oregon. Table 4 shows model performance statistics for the year 2016 across the measurement sites summarized in Fig. 2 for comparison to standard model performance criteria. PM<sub>2.5</sub> mass predictions during

summer months are in good agreement with measurements, but generally under-predicted during winter months. Portland and Eugene have population densities that are similar to Sacramento, CA, but the NEI per capita wood smoke emissions in the Oregon cities are a factor of 10–100 lower than CARB per capita wood smoke emissions in Sacramento, suggesting that wood smoke emissions in Oregon may be underestimated. Increasing wood smoke emissions by a factor of ~10 in the Portland area and ~100 in the Eugene area to be consistent with emissions rates in Sacramento significantly improves model performance but does not completely eliminate PM<sub>2.5</sub> under predictions in the winter season (see red lines in Fig. 2). This issue should not influence the analysis of public health benefits associated with the adoption of low CI transportation fuels, however. Therefore, the NEI is used to represent non-transportation sources in the following 2035 analysis. Corrections to the wood smoke emissions will be fully investigated in the next iteration of modeling when all sectors adopt measures to reduce emissions.

WRF four-dimensional Data Assimilation (FDDA) was not used in the 2017 basecase QA/QC simulation because FDDA cannot be used in the future year scenarios (no measurements). Previous studies have found that WRF configured without FDDA may overestimate wind speed and Planetary Boundary Layer (PBL) height, with stronger effects in the winter period than the summer period (Li et al., 2016; Tran et al., 2018). Increased ventilation can cause an under-prediction of pollutant concentrations. It is possible that wind-speed over-predictions could contribute to the under-prediction of concentrations in Oregon cities during the winter season. This issue could potentially influence the magnitude of the concentration changes within each emissions scenario, but not the directionality of those changes.

Routine PM<sub>2.5</sub> measurements in Oregon do not collect source apportionment information and so there is no way to directly evaluate the accuracy of the source apportionment results predicted by the UCD/CIT model in the current study. The agreement between predicted and measured total PM<sub>2.5</sub> mass concentrations builds confidence in the accuracy of the model inputs, and previous studies have verified the accuracy of the UCD/CIT source apportionment predictions in California (see for example Hu et al., 2015, 2017; Yu et al., 2019).

The time series of primary PM<sub>2.5</sub> mass concentrations associated with on-road gasoline vehicles (tracer 1) and on-road diesel vehicles (tracer 3) during the year 2016 are shown in Fig. S15. Concentrations for the primary PM<sub>2.5</sub> mass associated with these on-road sources generally increase during the colder winter months due to reduced atmospheric mixing and lower planetary boundary layer height. These seasonal patterns will persist in future years.

Spatial patterns for all nine tracers for primary particulate matter associated with different source categories are presented in Fig. S13. On-road vehicle emissions account for ~20% of the primary airborne PM in urban areas such as Portland. These are the emissions that will change

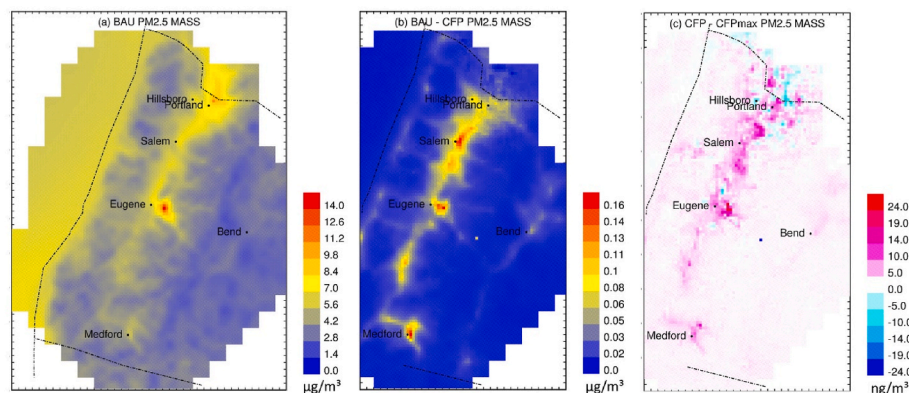


**Fig. 3.** (a) PM<sub>2.5</sub> mass concentration for BAU scenario ( $\mu\text{g m}^{-3}$ ), (b) the difference between BAU and CFP scenarios ( $\mu\text{g m}^{-3}$ ), and (c) the difference between CFP and CFP MAX scenarios ( $\text{ng m}^{-3}$ ).

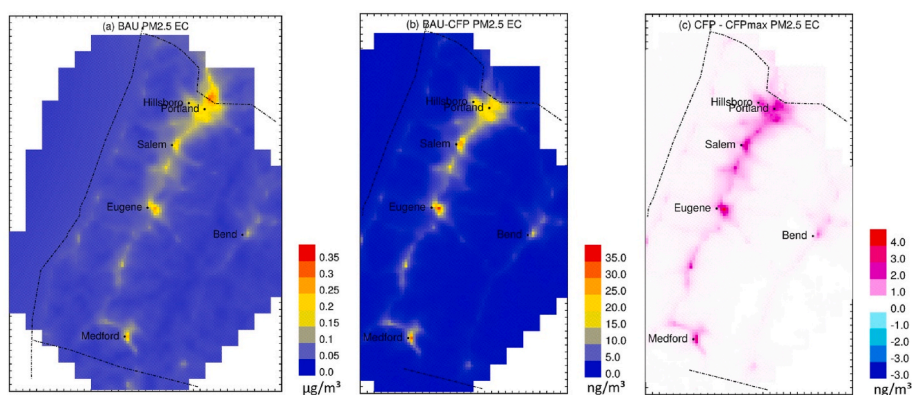


Fig. 4. (a) PM<sub>2.5</sub> EC concentration for BAU scenario ( $\mu\text{g m}^{-3}$ ), (b) the difference between BAU and CFP scenarios ( $\text{ng m}^{-3}$ ), and (c) the difference between CFP and CFP MAX scenarios( $\text{ng m}^{-3}$ ).

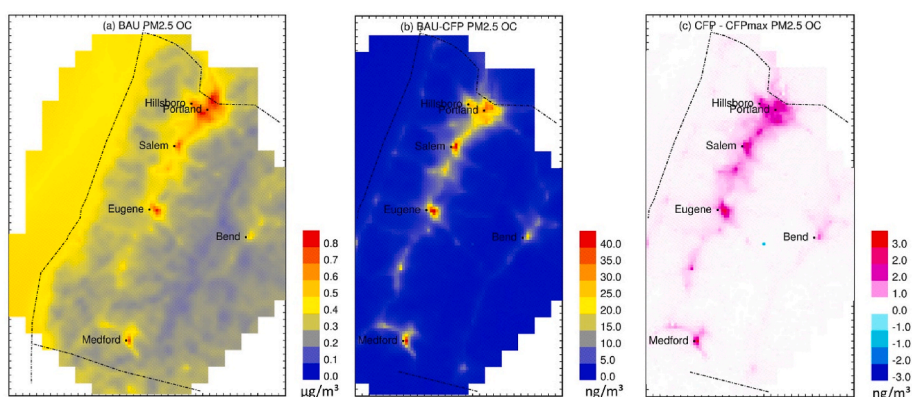


Fig. 5. (a) PM<sub>2.5</sub> OC concentration for BAU scenario ( $\mu\text{g m}^{-3}$ ), (b) the difference between BAU and CFP scenarios ( $\text{ng m}^{-3}$ ), and (c) the difference between CFP and CFP MAX scenarios( $\text{ng m}^{-3}$ ).

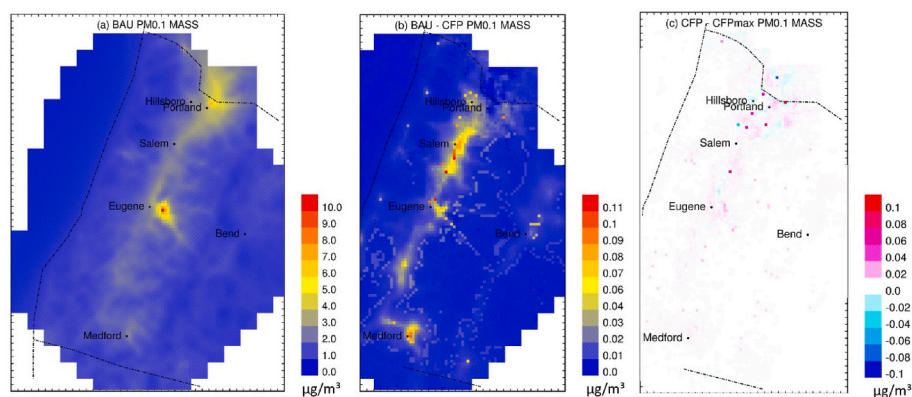


Fig. 6. (a) PM<sub>0.1</sub> mass concentration for BAU scenario ( $\mu\text{g m}^{-3}$ ), (b) the difference between BAU and CFP scenarios ( $\mu\text{g m}^{-3}$ ), and (c) the difference between CFP and CFP MAX scenarios( $\mu\text{g m}^{-3}$ ).

due to the adoption of low-carbon transportation fuels. The remaining primary particles are mainly associated with natural gas combustion, residential fuel combustion, and offroad diesel equipment. The relatively modest contribution from on-road vehicles in the 2016 simulation helps to frame expectations for the effects of low-carbon fuel adoption in future scenarios.

### 3.2. Future air quality simulations

#### 3.2.1. PM concentrations comparisons between BAU, CFP and CFP MAX scenarios

The change in total PM<sub>2.5</sub> mass, EC, OC and PM<sub>0.1</sub> mass (summed across all sources) was first analyzed since these pollutants determine how the adoption of low CI transportation fuel will affect total public health. Figs. 3–6 show long-term PM<sub>2.5</sub> total mass, EC, OC and PM<sub>0.1</sub> total mass concentrations in the 2035 BAU scenario (panel a) along with changes caused by the adoption of low-carbon transportation fuels in the

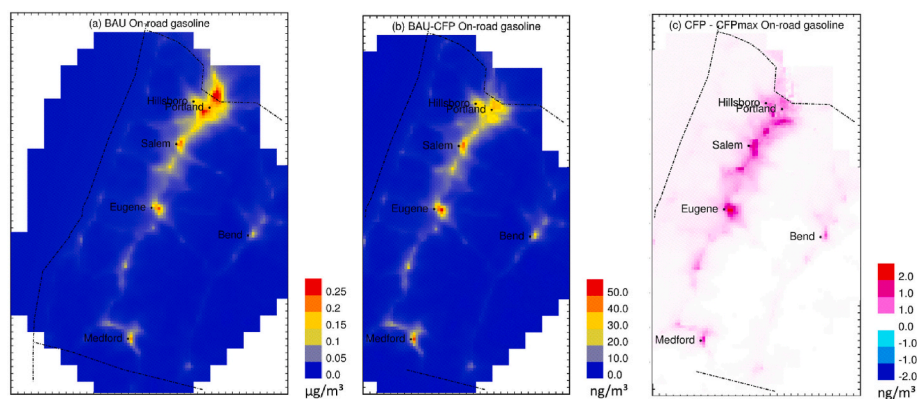


Fig. 7. (a) PM<sub>2.5</sub> on-road gasoline source concentration for BAU scenario ( $\mu\text{g m}^{-3}$ ), (b) the difference between BAU and CFP scenarios ( $\text{ng m}^{-3}$ ), and (c) the difference between CFP and CFP MAX scenarios ( $\text{ng m}^{-3}$ ).

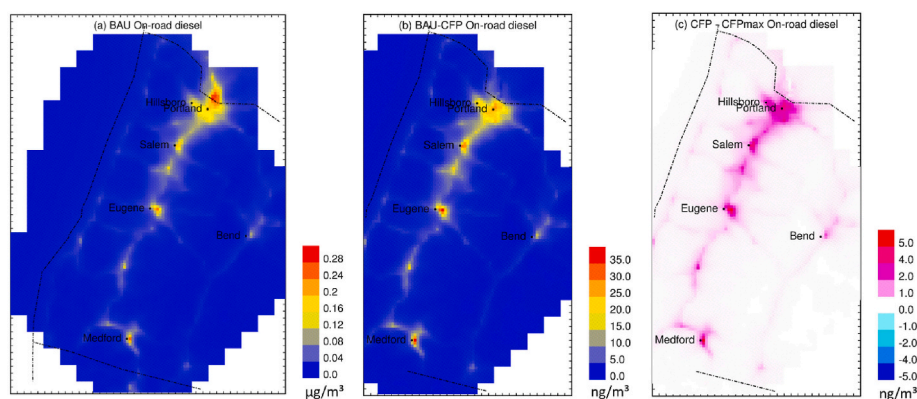


Fig. 8. (a) PM<sub>2.5</sub> on-road diesel source concentration for BAU scenario ( $\mu\text{g m}^{-3}$ ), (b) the difference between BAU and CFP scenarios ( $\text{ng m}^{-3}$ ), and (c) the difference between CFP and CFP MAX scenarios ( $\text{ng m}^{-3}$ ).

CFP and CFP MAX scenarios (panel b and c). PM total mass, EC and OC reductions occur mainly along the I-5 corridor connecting Portland, Eugene and Salem. PM<sub>2.5</sub> EC concentrations are predicted to decrease ~10–20%, PM<sub>2.5</sub> OC concentrations are predicted to decrease ~6–10% and PM<sub>0.1</sub> mass concentrations are predicted to decrease ~5–15% depending on location. PM<sub>2.5</sub> EC is strongly associated with on-road diesel engine emissions, but other sources make relatively larger contributions to PM<sub>2.5</sub> OC and PM<sub>0.1</sub> mass concentrations.

### 3.2.2. Mobile source PM comparisons between BAU, CFP and CFP MAX scenarios

Changes to predicted ambient concentrations of primary PM<sub>2.5</sub> mass associated with tailpipe emissions from on-road gasoline vehicles and on-road diesel vehicles were analyzed to further quantify the pollutants changes associated with mobile sources. Fig. 7 shows predicted changes to the primary ambient PM<sub>2.5</sub> mass associated with tailpipe emissions from on-road gasoline vehicles (tracer 1) between the BAU and CFP/CFP MAX scenarios. The greatest reductions of ~25% are predicted to occur in Salem and Eugene, while predicted concentrations in Portland decrease by a more modest ~10% (Fig. 7b). The concentration difference between the CFP and CFP MAX scenarios (Fig. 7c) is smaller than the concentration difference between the BAU and CFP scenarios (Fig. 7b).

Fig. 8 shows predicted changes to the concentration of primary PM<sub>2.5</sub> mass associated with tailpipe emissions from on-road diesel vehicles (tracer 3) between the BAU and CFP/CFP MAX scenarios. Diesel mobile emissions reductions of ~15% are apparent in major cities including Salem, Eugene, and Portland.

Reductions in primary PM<sub>2.5</sub> mass concentrations associated with

diesel vehicles (1.8%, compare Fig. 8c–b) are larger than corresponding reductions for gasoline vehicles (0.5%, compare Fig. 7c–b) under the CFP MAX scenario vs. the CFP scenario. This result reflects the utilization of different fuels in the two scenarios. The CFP scenario has significant ZEV market penetration, driven by the adoption of California's Advanced Clean Cars, Advanced Clean Trucks and Advanced Clean Fleets rules. This causes a significant transition from gasoline internal combustion engine (ICE) vehicles in the light-duty sector towards electric vehicles (EVs), and a smaller but still significant transition towards EVs in the medium and heavy-duty sector. These transitions reduce CI and successfully attain the 25% target specified in Executive Order 20-04 without requiring any significant growth in the consumption of biodiesel and renewable diesel beyond historical trends.

The CFP MAX scenario further reduces CI by expanding the consumption of renewable diesel in medium and heavy-duty vehicles. An additional 25% of the fossil diesel demand is replaced by renewable diesel and CNG in the CFP MAX scenario. Renewable diesel reduces life cycle GHG emissions when displacing petroleum, however, renewable diesel offers minimal air quality benefit when used in modern diesel engines equipped with diesel particulate filters (DPFs) and selective catalytic reduction (SCR) systems. Both of these systems are required in Oregon for post-2010 model year diesel vehicles. Therefore, the pollutant concentration fields predicted under the CFP and CFP MAX scenarios are similar, even though the life-cycle GHG emissions are significantly lower in the CFP MAX scenario.

It should be noted that tire and brake wear emissions were held constant in the CFP scenario and the CFP MAX scenario, but these emissions could be targeted for reductions in the future mitigation policies.

**Table 5**  
BenMAP Health Impact Analysis between BAU and CFP/CFP MAX scenarios.

Year	Scenario	Mortality	Mortality per 1,000,000	Economic Value
<b>PM2.5 MASS<sup>1</sup></b>				
2035	BAU	608.04	242.46	(cost) \$ 4,234,770,176
2035	CFP saving	12.12	4.83	\$ 84,411,920
2035	CFP MAX saving	12.56	5.01	\$ 87,779,543
<b>Tracer 1 – On-road Gasoline<sup>2</sup></b>				
2035	BAU	21.16	8.44	(cost) \$ 147,378,448
2035	CFP saving	3.42	1.36	\$ 23,807,160
2035	CFP MAX saving	3.50	1.39	\$ 24,346,360
<b>Tracer 3 – On-road Diesel<sup>3</sup></b>				
2035	BAU	19.79	7.89	(cost) \$ 137,825,424
2035	CFP saving	2.49	0.99	\$ 17,331,380
2035	CFP MAX saving	2.81	1.12	\$ 19,573,342

<sup>1</sup>Primary and secondary PM; <sup>2,3</sup>primary tailpipe PM only.

**3.2.3. Health impact comparison between BAU and CFP, CFP MAX scenarios**

The results presented in the previous sections summarize total PM concentrations under different emissions scenarios, including separate tracking of primary PM (emitted directly from the vehicle) and secondary PM (formed by reactions of gas-phase pollutants in the atmosphere). Table 5 shows the BenMAP health impact analysis based on the changes to total PM<sub>2.5</sub> mass, including primary and secondary PM<sub>2.5</sub> and primary PM<sub>2.5</sub> mass by itself associated with on-road vehicles summarized in Figs. 3, Figs. 7 and 8. BenMAP (configured with the (Krewski et al., 2009) health damage function) predicts 242 excess deaths per year

for every 1,000,000 people in the 2035 BAU scenario because of exposure to concentrations of PM<sub>2.5</sub> total mass from all sources, including transportation and non-transportation sources, relative to the assumed background concentrations.

Primary PM<sub>2.5</sub> emitted from the tailpipes of on-road gasoline vehicles accounts for an estimated eight excess deaths per 1,000,000 people, and primary PM emitted from the tailpipes of on-road diesel vehicles accounts for an estimated eight excess deaths per 1,000,000 people in the 2035 BAU scenario. The air pollution mortality estimates decrease in proportion to the concentration reductions in the low-carbon transportation fuel scenarios. Adoption of low carbon fuels (CFP and CFP

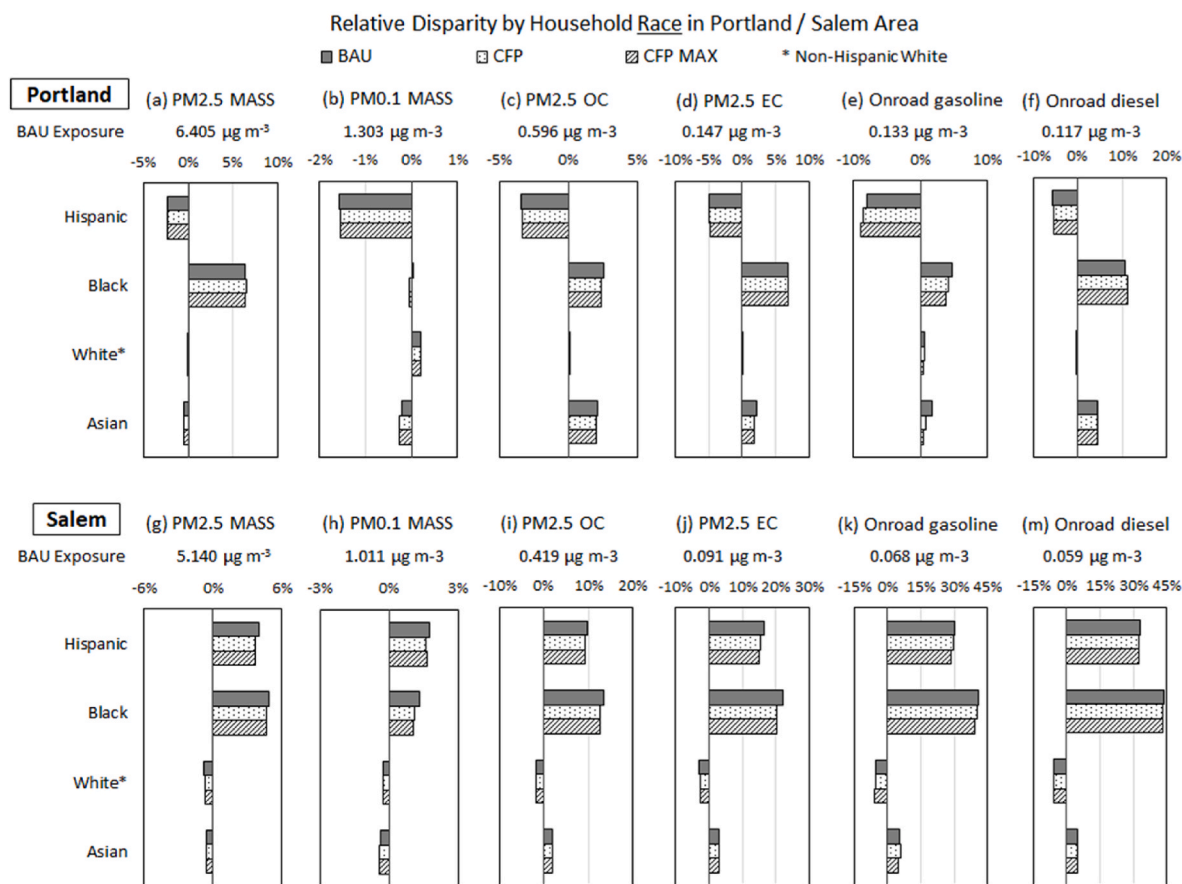


**Fig. 9.** Relative disparity from population average exposure concentrations for 6 PM components in year 2035 based on household race/ethnicity. Shaded gray (BAU)/dotted (CFP)/striated (CFP MAX) bars represent relative household weighted concentrations compared to total population average exposure. The average exposure concentration in the BAU scenario is listed at the top of each sub-panel.

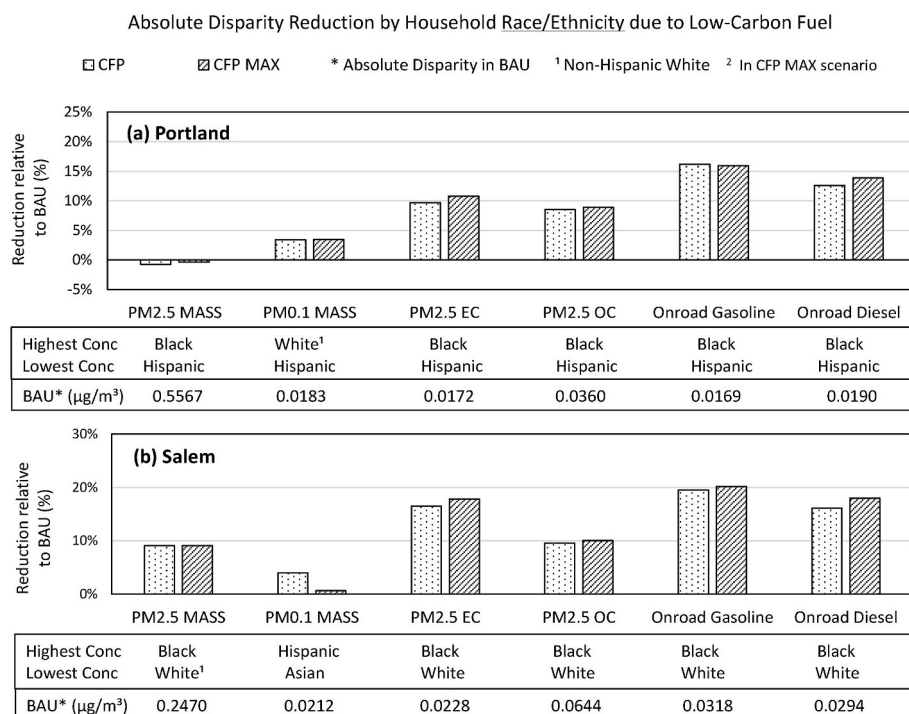


**Fig. 10.** Absolute disparity in household ethnicity/race exposure concentrations for 6 PM components in the year 2035. The boxed row represents changes to absolute disparity value relative to BAU, and corresponding highest exposure group and lowest exposure group. Dotted (CFP)/striated (CFP MAX) bar represent percentage changes compared to BAU.

MAX) reduces mortality associated with primary PM emitted from gasoline vehicles by ~ 16% and mortality associated with primary PM emitted from diesel vehicles by ~ 12.5%.

Attribution of mortality from secondary PM can be estimated by comparing total mortality under the 2035 CFP and 2035 CFP MAX scenarios to mortality in the 2035 BAU scenario, and then excluding the impacts of primary PM. In both scenarios, secondary PM accounts for approximately 50% of the total health savings associated with the adoption of low-carbon transportation fuels.

### 3.3. Environmental justice (EJ) analysis between BAU and CFP, CFP MAX scenarios

#### 3.3.1. Exposure disparity by household race/ethnicity

Disparities in exposure concentrations were analyzed for four different household race/ethnicity groups: i) non-Hispanic White; ii) Asian alone; iii) Black and African American; iv) Hispanic or Latino, regardless of race, for 6 PM components, including PM<sub>2.5</sub> mass, EC, OC, primary particles from on-road gasoline tailpipes, primary particles from on-road diesel tailpipes, and PM<sub>0.1</sub> mass. Fig. 9 shows relative exposure disparities as well as average exposure in the BAU scenario for these pollutants. Fig. 10 shows absolute disparities in the BAU scenario and changes to disparity under the 2035 CFP and CFP MAX scenarios for the six pollutants. The absolute exposure disparity concentrations in the BAU scenario are listed along the bottom of the figure, while the disparity reduction in the CFP and CFP MAX scenarios relative to BAU scenario are shown in the bar chart. Household Population Weighted Concentrations (HPWCs) used for Figs. 9 and 10 can be found in Figs. S16–17. As expected, pollutant exposures are generally higher in the BAU scenario than the two low-carbon transportation fuel scenarios, especially for pollutants associated with mobile sources (PM<sub>2.5</sub> EC, on-road gasoline and on-road diesel tracers). Exposures in the CFP and CFP MAX scenarios are similar, which is consistent with the minor changes in the emissions associated with these scenarios. Exposures to PM<sub>2.5</sub> total mass, OC, and PM<sub>0.1</sub> total mass are similar in the 2035 BAU,

2035 CFP, and 2035 CFP MAX scenarios because these components are mainly associated with non-transportation sources that were not controlled in the current study.

Exposures to pollutants emitted directly from mobile sources (PM<sub>2.5</sub> EC, on-road gasoline and on-road diesel tracers) have larger relative disparities than exposures to PM<sub>2.5</sub> total mass, OC, and PM<sub>0.1</sub> total mass (Fig. 9). Around 80% of the population in the cities of Portland and Salem is non-Hispanic White, and so it is expected that exposure concentrations for this group will be close to the average exposure for the total population in the study region. This finding is illustrated most clearly in Fig. 9, where the relative exposure disparities for the non-Hispanic White residents are close to zero. Relative exposure disparities for other race/ethnicity groups diverge from the total population average exposures with the details depending on location. This pattern differs from trends in several California cities (Li et al., 2022a) and at other locations across the US (Banzhaf et al., 2019; Colmer et al., 2020; Di et al., 2017; Mikati et al., 2018; Rosofsky et al., 2018; Tessum et al., 2021) where White residents are generally exposed to lower concentrations and minorities are exposed to higher concentrations.

In Portland (Fig. 9(a-f)), Hispanic or Latino residents are exposed to the lowest concentrations for all 6 PM pollutants. Black and African American residents are exposed to significantly higher-than-average PM concentrations except for PM<sub>0.1</sub> mass. This result reflects the population distribution around Portland. The majority of the Black & African American residents live Northeast of Portland (Fig. S3), which is close to the urban core. However, Hispanic residents in Portland live outside of the urban core, where concentrations are significantly lower (see Fig. S4). In Salem (Fig. 9(g-m)), Hispanic and Black residents experience the highest PM exposure concentrations. Overall, the exposure disparities in Oregon reflect the somewhat uniform distribution of non-Hispanic White residents across the study region, including in urban core areas, while other race/ethnicity groups live further from the urban core (lower concentrations) or closer to major transportation corridors (higher concentrations).

Exposure disparities between different race/ethnicity groups

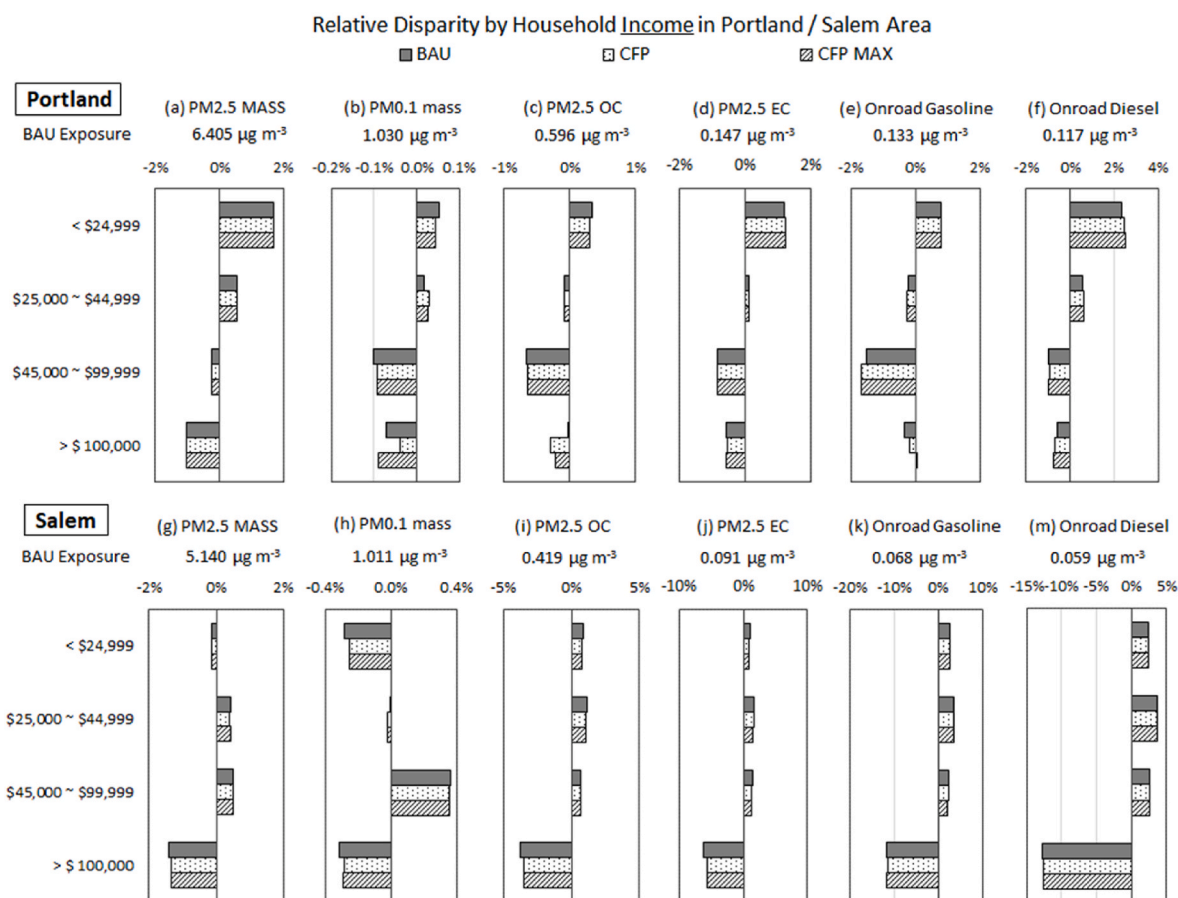


**Fig. 11.** Relative disparity from population-average exposure concentration for 6 PM components in year 2035 based on household income. Shaded gray (BAU)/dotted (CFP)/striated (CFP MAX) bars represent relative income weighted concentrations compared to total population average exposure. The average exposure concentration in the BAU scenario is listed at the top of each sub-panel.

decrease under the future scenarios that adopt low-carbon transportation fuels for most pollutants (Fig. 10). Exposure disparities for pollutants directly associated with transportation sources (EC, primary particles emitted from gasoline and diesel tailpipes) decrease by 10–15% in Portland and 15–20% in Salem under the low carbon scenarios. Exposure disparities for  $PM_{2.5}$  OC decrease by 8–10% in Portland and Salem. Exposure disparity to  $PM_{2.5}$  total mass also decreases by 10% in Salem, but remains approximately constant in Portland when low carbon transportation fuels are adopted. The  $PM_{2.5}$  mass absolute disparity in Portland is  $0.5567 \mu\text{g}/\text{m}^3$ . Exposure disparities in Portland for on-road tracers are  $0.0169 \mu\text{g}/\text{m}^3$  for gasoline and  $0.019 \mu\text{g}/\text{m}^3$  for diesel (<3% of the total  $PM_{2.5}$  mass disparity). Reductions of transportation-related exposure disparities therefore won't significantly affect total  $PM_{2.5}$  mass exposure disparity in Portland. Adoption of low-carbon fuels in the CFP scenario decreases  $PM_{0.1}$  exposure disparity by ~4% in Portland and Salem. Some of these reductions in  $PM_{0.1}$  exposure disparity are lost in the transition from the CFP scenario to the CFP MAX scenario. The CFP MAX scenario includes more heavy duty CNG vehicles and renewable diesel vehicles than the CFP scenario. Natural gas combustion generates a greater fraction of ultrafine particles with diameters  $<0.1 \mu\text{m}$  ( $PM_{0.1}$ ) (Yu et al., 2019) even though the related  $PM_{2.5}$  emissions decrease. As discussed in Section 2.5, many Hispanic residents in Salem live close to the I-5 corridor, which increases their exposure to emissions from on-road heavy-duty vehicles.

### 3.3.2. Exposure disparity by household income

Fig. 11 shows the calculated relative exposure disparity among the four household income categories for  $PM_{2.5}$  mass, EC, OC, primary PM from the tailpipes of on-road gasoline vehicles, primary PM from the

tailpipes of on-road diesel vehicles, and  $PM_{0.1}$  mass. Household Population Weighted Concentrations (HPWCs) used in Fig. 11 are displayed in Figs. S18–19. In general, relative exposure disparity by income is smaller than disparities associated with race/ethnicity. Exposure disparities for transportation related pollutants ( $PM_{2.5}$  EC, primary PM from the tailpipes of on-road gasoline vehicles, primary PM from the tailpipes of on-road diesel vehicles) are larger than exposure disparities for  $PM_{2.5}$  mass and  $PM_{2.5}$  OC. Lower income households in Portland and Salem are exposed to higher air pollution concentrations in all scenarios, while higher income households are exposed to lower concentrations. The relative trend of increasing exposure concentrations at lower income levels in Portland and Salem is consistent with the national trend (Banzhaf et al., 2019; Bell and Ebisu, 2012; Colmer et al., 2020; Di et al., 2017; Mikati et al., 2018). Trends in Portland are slightly complicated by the fact that many high-income households live in the city core, leading to increasing exposure concentrations. The lowest exposure group in Portland is the second-highest income category ( $\$45,000 \sim \$99,999$ ), instead of the highest income category ( $>\$100,000$ ). The highest income group in Salem lives outside of the urban core and away from Highway I-5, leading to significantly lower exposure concentrations. The first three income categories in Salem do not have significant spatial patterns, which results in close-to-average exposure concentrations.

Fig. 12 displays disparities between the highest exposure group and the lowest exposure group for the 6 PM pollutants displayed in Fig. 11. The absolute exposure disparity concentrations in the BAU scenario are listed along the bottom of the figure, while the disparity reduction in the CFP and CFP MAX scenarios relative to BAU scenario are shown in the bar chart.  $PM_{2.5}$  mass, OC exposure disparities change by less than 8% in Portland and 10% in Salem due to adoption of low-carbon

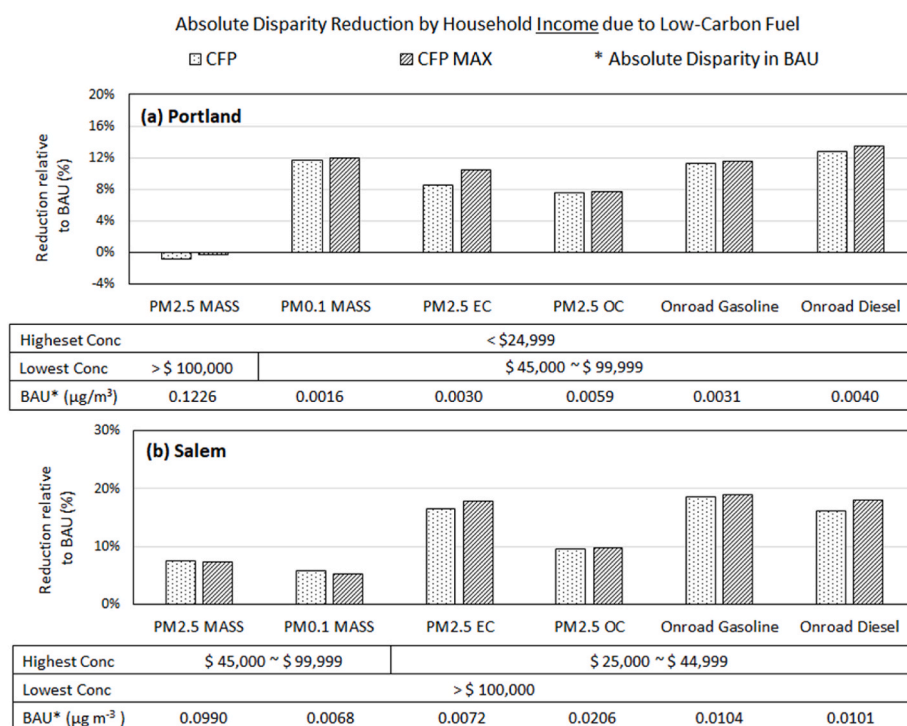


**Fig. 12.** Absolute disparity in household income exposure concentrations for 6 PM components in the year 2035. The boxed row represents changes to absolute disparity value relative to BAU, and corresponding highest exposure group and lowest exposure group. Dotted (CFP)/striated (CFP MAX) bar represent percentage changes compared to BAU.

transportation fuels because these components are mainly associated with non-transportation sources. Exposure disparities for  $\text{PM}_{2.5}$  EC, primary particles associated with tailpipe emissions from on-road gasoline vehicles, and primary particles associated with tailpipe emissions from on-road diesel vehicles decreased by ~10%, ~12% and ~14% in Portland and by ~18%, ~19% and ~18% in Salem, respectively. The absolute disparity in  $\text{PM}_{0.1}$  exposure decreased by ~12% in Portland and ~6% in Salem.

#### 4. Discussion and conclusions

Population exposure to  $\text{PM}_{2.5}$  total mass, EC, OC, on-road gasoline/diesel and  $\text{PM}_{0.1}$  in Oregon decreased in future year 2035 scenarios that adopted GHG emissions mitigation strategies consistent with the proposed expansion of Oregon’s Clean Fuels Program relative to a BAU scenario. Technologies such as electric vehicles and biofuels reduced emissions of criteria air pollutants such as PM,  $\text{NO}_x$ , and  $\text{SO}_x$ , as well as GHGs. PM reductions mainly occurred along the I-5 corridor, especially in the major cities Eugene and Salem. Adoption of low carbon fuels reduced  $\text{PM}_{2.5}$  EC concentrations by ~10–20%,  $\text{PM}_{2.5}$  OC concentrations by ~6–10% and  $\text{PM}_{0.1}$  mass concentrations by ~5–15% depending on location. Concentrations of primary PM emitted directly from the tailpipes of on-road gasoline vehicles decreased by ~11% in Salem and Eugene and ~10% in Portland. Concentrations of primary PM emitted from the tailpipes of on-road diesel vehicles decreased by ~15% in the same cities. The majority of the PM reductions were achieved under a scenario that lowered GHG emissions by 25%. A more aggressive scenario that lowered GHG emissions by 37% through the further adoption of biofuels in diesel engines resulted in only minor amounts of additional PM reduction because the modern diesel engines in the year 2035 fleet were already equipped with advanced emissions control technology. Concentrations of pollutants other than PM decreased under the modeled compliance scenarios as well, but these generally had minimal health impacts.

Standard epidemiological associations predict 242 annual deaths per

1,000,000 population in Oregon from exposure to total  $\text{PM}_{2.5}$  mass from all sources in the 2035 BAU scenario. Primary PM emitted from on-road gasoline vehicles and on-road diesel vehicles each account for approximately 8 excess deaths per 1,000,000 each year. Adoption of low carbon transportation fuels reduces excess mortality by approximately 5 deaths per 1,000,000 people each year. Reductions in primary and secondary PM each account for approximately 50% of this avoided mortality. Adoption of low carbon fuels reduces mortality associated with primary PM emitted from gasoline vehicles by ~16% and mortality associated with primary PM emitted from diesel vehicles by ~12.5%.

Exposure trends across different race/ethnicity groups reflect the size and geographical distribution of those groups. More than 80% of the population in Portland and Salem is Non-Hispanic White, and so these residents experience exposure concentrations very close to the population average. Relative exposure disparities for other race/ethnicity groups diverge from the total population average exposures with the details depending on location. Black and African Americans are the highest exposure group in both Portland and Salem. Black residents in Portland live close to the urban core, while Black residents in Salem live close to transportation corridors. In Portland, Hispanic or Latino residents are exposed to the lowest exposure concentrations because they live outside of urban core and away from major transportation corridors. However, in Salem, Hispanic or Latino residents are exposed to higher-than-average concentrations because they live close to Interstate 5. It is important to note that these exposure calculations have a spatial resolution of 4 km, which may not resolve pollutant gradients near freeways and major surface streets. Studies carried out in California show that exposure patterns identified with 4 km spatial resolution are consistent with exposure patterns quantified at 1 km and 0.25 km spatial resolution (Li et al., 2022a).

Exposure disparities across different income groups are smaller than exposure disparities based on race/ethnicity. In general, lower income households in Portland and Salem are exposed to higher air pollution concentrations in all scenarios, while higher income households are exposed to lower concentrations. Trends in Portland are slightly

complicated by the fact that many high-income households live in the city core, leading to increasing exposure concentrations for this wealthy group. The lowest exposure group in Portland is the second-highest income category (\$45,000 ~ \$99,999), instead of the highest income category (>\$100,000).

Adoption of low-carbon transportation fuels reduces exposure disparity based on race/ethnicity by 10–18% for PM<sub>2.5</sub> elemental carbon (EC) and 14–20% for primary tailpipe PM. Reductions in exposure disparity based on race/ethnicity are less than 10% for PM<sub>2.5</sub> mass, OC, and PM<sub>0.1</sub> mass that have major sources other than transportation. This pattern is to be expected because the purpose of this study was to characterize the impacts of a transportation-focused policy, the CFP, while holding all other sources at existing levels. The majority of the disparity reduction was achieved by the 25% GHG reduction scenario, with only minor additional benefits associated with the 37% GHG reduction scenario.

The current study suggests that the proposed expansion of Oregon's Clean Fuels Program is likely to produce a significant air quality benefit that reduces excess mortality for all residents and simultaneously reduces PM<sub>2.5</sub> exposure disparities between different socio-economic groups. This aligns with the prevalent consensus within the transportation and air quality research literature that displacing petroleum-based transportation fuels for non-petroleum alternatives typically yields improved air quality. Adoption of clean fuels in the transportation sector, however, will not completely eliminate exposure disparities for all groups and all pollutants.

#### CRedit authorship contribution statement

**Yiting Li:** created emissions inventories, performed model simulations, and wrote first, Writing – original draft, of manuscript. **Guihua Wang:** created mobile emissions inventories. **Colin Murphy:** Formal analysis, GHG control policies and technology changes inherent in future scenarios. **Michael J. Kleeman:** designed the study, created models used to predict future air quality, and revised the manuscript.

#### Declaration of competing interest

The authors declare that they have no known competing financial interests or personal relationships that could have appeared to influence the work reported in this paper.

#### Data availability

Data will be made available on request.

#### Acknowledgement

This research was supported by the Oregon Department of Environmental Quality (DEQ) under Project #162-20. The views expressed in this article are those of the authors and do not represent the views or policies of the Oregon DEQ.

#### Appendix A. Supplementary data

Supplementary data to this article can be found online at <https://doi.org/10.1016/j.atmosenv.2023.119582>.

#### References

- Anderson, C.M., Kissel, K.A., Field, C.B., Mach, K.J., 2018. Climate change mitigation, air pollution, and environmental justice in California. *Environ. Sci. Technol.* 52 (18), 10829–10838. <https://doi.org/10.1021/acs.est.8b00908>.
- Banzhaf, S., Ma, L., Timmins, C., 2019. Environmental justice: the economics of race, place, and pollution. *J. Econ. Perspect.* 33 (1), 185–208. <https://doi.org/10.1257/jep.33.1.185>.

- Bartlett, C.J.S., Betts, W.E., Booth, M., Giavazzi, F., Guttman, H., Heinze, P., M, R.F., Hutcheson, R.C., 1992. Diesel Fuel Aromatic Content and its Relationship with Emissions from Diesel Engines. *Report No. 92/54*.
- Bell, M.L., Ebisu, K., 2012. Environmental inequality in exposures to airborne particulate matter components in the United States. *Environ. Health Perspect.* 120 (12), 1699. <https://doi.org/10.1289/EHP.1205201>.
- Bravo, M.A., Anthopoulos, R., Bell, M.L., Miranda, M.L., 2016. Racial isolation and exposure to airborne particulate matter and ozone in understudied US populations: environmental justice applications of downscaled numerical model output. *Environ. Int.* 92 (93), 247–255. <https://doi.org/10.1016/j.envint.2016.04.008>.
- California Air Resource Board, 2021. California Greenhouse Gas Emission Inventory. <https://ww2.arb.ca.gov/ghg-inventory-data>.
- Choma, E.F., Evans, J.S., Gomez-Ibanez, J.A., Di, Q., Schwartz, J.D., Hammitt, J.K., Spengler, J.D., 2021. Health benefits of decreases in on-road transportation emissions in the United States from 2008 to 2017. *Proc. Natl. Acad. Sci. U.S.A.* 118 (51) [https://doi.org/10.1073/PNAS.2107402118/SUPPL\\_FILE/PNAS.2107402118.SD05.CSV](https://doi.org/10.1073/PNAS.2107402118/SUPPL_FILE/PNAS.2107402118.SD05.CSV).
- Churg, A., Brauer, M., 2012, 6. Human Lung Parenchyma Retains PM<sub>2.5</sub>, vol. 155, pp. 2109–2111. <https://doi.org/10.1164/AJRCM.155.6.9196123>.
- Cohen, A.J., Anderson, R.H., Ostro, B., Pandey, K., Krzyzanowski, M., Künzli, N., Gutschmidt, K., Pope, A., Romieu, I., Samet, J.M., Smith, K., 2005. The global burden of disease due to outdoor air pollution. *J. Toxicol. Environ. Health, Part A* 68, 1301–1307. <https://doi.org/10.1080/15287390590936166>.
- Colmer, J., Hardman, I., Shimshack, J., Voorheis, J., 2020. Disparities in PM<sub>2.5</sub> air pollution in the United States. *Science* 369 (6503), 575–578. <https://doi.org/10.1126/SCIENCE.AAZ9353>.
- Cushing, L., Faust, J., August, L.M., Cendak, R., Wieland, W., Alexeeff, G., 2015. Racial/ethnic disparities in cumulative environmental health impacts in California: evidence from a statewide environmental justice screening tool (CalEnviroScreen 1.1). *American J. Public Health* 105 (11), 2341–2348. <https://doi.org/10.2105/AJPH.2015.302643>.
- Di, Q., Wang, Y., Zanobetti, A., Wang, Y., Koutrakis, P., Choirat, C., Dominici, F., Schwartz, J.D., 2017. Air pollution and mortality in the medicare population. *N. Engl. J. Med.* 376 (26), 2513–2522. <https://doi.org/10.1056/NEJMoa1702747>.
- Durbin, T.D., Karavalakis, G., Johnson, K., McCaffery, C., Zhu, H., Li, H., 2021. Low Emission Diesel (LED) Study: Biodiesel and Renewable Diesel Emissions in Legacy and New Technology Diesel Engines - Final Report.
- Gent, P., Donner, L., Lawrence, D., Gent, P.R., Danabasoglu, G., Donner, L.J., Holland, M. M., Hunke, E.C., Jayne, S.R., Lawrence, D.M., Neale, R.B., Rasch, P.J., Vertenstein, M., Worley, P.H., Yang, Z.-L., Zhang, M., 2011. The community climate system model version 4 OCEANFILMS view project dust emission modeling view project the community climate system model version 4. *Article J. Climate.* <https://doi.org/10.1175/2011JCLI4083.1>.
- Giglio, L., Randerson, J.T., Werf, G.R., 2013. Analysis of daily, monthly, and annual burned area using the fourth-generation global fire emissions database (GFED4). *J. Geophys. Res.: Biogeosciences* 118, 317–328. <https://doi.org/10.1002/jgrg.20042>.
- Goodkind, A.L., Tessum, C.W., Coggins, J.S., Hill, J.D., Marshall, J.D., 2019. Fine-scale damage estimates of particulate matter air pollution reveal opportunities for location-specific mitigation of emissions. *Proc. Natl. Acad. Sci. U.S.A.* 116 (18), 8775–8780. <https://doi.org/10.1073/pnas.1816102116>.
- Guenther, A.B., Jiang, X., Heald, C.L., Sakulyanontvittaya, T., Duhl, T., Emmons, L.K., Wang, X., 2012. The model of emissions of gases and aerosols from nature version 2.1 (MEGAN2.1): an extended and updated framework for modeling biogenic emissions. *Geosci. Model Dev. (GMD)* 5 (6), 1471–1492. <https://doi.org/10.5194/GMD-5-1471-2012>.
- Hu, J., Zhang, H., Chen, S.-H., Wiedinmyer, C., Vandenberghe, F., Ying, Q., Kleeman, M. J., 2014. Predicting primary PM<sub>2.5</sub> and PM<sub>0.1</sub> trace composition for epidemiological studies in California. *Environ. Sci. Technol.* 48, 4971–4979. <https://doi.org/10.1021/es404809j>.
- Hu, J., Zhang, H., Ying, Q., Chen, S.-H., Vandenberghe, F., Kleeman, M.J., 2015. Long-term particulate matter modeling for health effect studies in California – Part 1: model performance on temporal and spatial variations. *Atmos. Chem. Phys.* 15, 3445–3461. <https://doi.org/10.5194/acp-15-3445-2015>.
- Hu, J., Jathar, S., Zhang, H., Ying, Q., Chen, S.-H., Cappa, C.D., Kleeman, M.J., 2017. Long-term particulate matter modeling for health effect studies in California – Part 2: concentrations and sources of ultrafine organic aerosols. *Atmos. Chem. Phys.* 17, 5379–5391. <https://doi.org/10.5194/acp-17-5379-2017>.
- ICF, 2021. 2021 illustrative compliance scenarios final report. <https://www.oregon.gov/deq/ghgp/Documents/cfpilluCompScenD.pdf>.
- Kleeman, M.J., Cass, G.R., Eldering, A., 1997. Modeling the airborne particle complex as a source-oriented external mixture. *J. Geophys. Res. Atmos.* 102 (1984–2012), 21355–21372. <https://doi.org/10.1029/97jd01261>.
- Krewski, D., Jerrett, M., Burnett, R.T., Ma, R., Hughes, E., Shi, Y., Turner, M.C., Newbold, B., Ramsay, T., Ross, Z., Shin, H., Tempalski, B., 2009. Extended Follow-Up and Spatial Analysis of the American Cancer Society Study Linking Particulate Air Pollution and Mortality.
- Lelieveld, J., Evans, J.S., Fnais, M., Giannadaki, D., Pozzer, A., 2015. The contribution of outdoor air pollution sources to premature mortality on a global scale. *Nature* 525 (7569), 367–371. <https://doi.org/10.1038/nature15371>.
- Lepeule, J., Laden, F., Dockery, D., Schwartz, J., 2012. Chronic exposure to fine particles and mortality: an extended follow-up of the harvard six cities study from 1974 to 2009. *Environ. Health Perspect.* 120 (7), 965. <https://doi.org/10.1289/EHP.1104660>.

- Lewis, F., Marshall, M., Andrew, B., Qian, W., Chris, Y., 2019. Technology and Fuel Transition Scenarios to Low Greenhouse Gas Futures for Cars and Trucks in California. <https://escholarship.org/uc/item/8wn8920p>.
- Li, X., Choi, Y., Czader, B., Roy, A., Kim, H., Lefler, B., Pan, S., 2016. The impact of observation nudging on simulated meteorology and ozone concentrations during DISCOVER-AQ 2013 Texas campaign. *Atmos. Chem. Phys.* 16 (5), 3127–3144. <https://doi.org/10.5194/ACP-16-3127-2016>.
- Li, Y., Rodier, C., Lea, J.D., Harvey, J., Kleeman, M.J., 2021. Improving spatial surrogates for area source emissions inventories in California. *Atmos. Environ.* 247, 117665 <https://doi.org/10.1016/j.atmosenv.2020.117665>.
- Li, Y., Kumar, A., Hamilton, S., Lea, J.D., Harvey, J., Kleeman, M.J., 2022a. Optimized environmental justice calculations for air pollution disparities in Southern California. *Heliyon* 8 (10), e10732. <https://doi.org/10.1016/J.HELIYON.2022.E10732>.
- Li, Y., Kumar, A., Li, Y., Kleeman, M.J., 2022b. Adoption of Low-Carbon Fuels Reduces Race/Ethnicity Disparities in Air Pollution Exposure in California. *Science of The Total Environment*, 155230. <https://doi.org/10.1016/J.SCITOTENV.2022.155230>.
- Liu, J., Clark, L.P., Bechle, M.J., Hajat, A., Kim, S.Y., Robinson, A.L., Sheppard, L., Spiro, A.A., Marshall, J.D., 2021. Disparities in air pollution exposure in the United States by race/ethnicity and income, 1990-2010. *Environ. Health Perspect.* 129 (12) <https://doi.org/10.1289/EHP8584> undefined-undefined.
- Mahla, S.K., Dhir, A., Gill, K.J.S., Cho, H.M., Lim, H.C., Chauhan, B.S., 2018. Influence of EGR on the simultaneous reduction of NOx-smoke emissions trade-off under CNG-biodiesel dual fuel engine. *Energy* 152, 303–312. <https://doi.org/10.1016/J.ENERGY.2018.03.072>.
- Mazzone, D., Witcover, J., Murphy, C., Org, E., 2021. UC Davis Research Reports Title Multijurisdictional Status Review of Low Carbon Fuel Standards Permalink. <https://doi.org/10.7922/G2SN0771>.
- Mikati, I., Benson, A.F., Luben, T.J., Sacks, J.D., Richmond-Bryant, J., 2018. Disparities in distribution of particulate matter emission sources by race and poverty status. *American J. Public Health* 108 (4), 480–485. <https://doi.org/10.2105/AJPH.2017.304297>.
- Miranda, M.L., Edwards, S.E., Keating, M.H., Paul, C.J., 2011. Making the environmental justice grade: the relative burden of air pollution exposure in the United States. *Int. J. Environ. Res. Publ. Health* 8 (6), 1755–1771. <https://doi.org/10.3390/ijerph8061755>.
- Oregon, 2018. Department of Environmental Quality : Oregon Greenhouse Gas Sector-Based Inventory Data : Air Quality Programs : State of Oregon. <https://www.oregon.gov/deq/aq/programs/Pages/GHG-Inventory.aspx>.
- Perlin, S.A., Setzer, R.W., Creason, J., Sexton, K., 2002. Distribution of industrial air emissions by income and race in the United States: an approach using the toxic release inventory. *Environ. Sci. Technol.* 29 (1), 69–80. <https://doi.org/10.1021/ES00001A008>.
- Pinkerton, K.E., Green, F.H.Y., Saiki, C., Vallyathan, V., Plopper, C.G., Gopal, V., Hung, D., Bahne, E.B., Lin, S.S., Ménache, M.G., Schenker, M.B., 2000. Distribution of particulate matter and tissue remodeling in the human lung. *Environ. Health Perspect.* 108 (11), 1063–1069. <https://doi.org/10.1289/EHP.001081063>.
- Qian, Y., Qiu, Y., Zhang, Y., Lu, X., 2017. Effects of different aromatics blended with diesel on combustion and emission characteristics with a common rail diesel engine. *Appl. Therm. Eng.* 125, 1530–1538. <https://doi.org/10.1016/J.APPLTHERMALENG.2017.07.145>.
- Rosofsky, A., Levy, J.I., Zanutti, A., Janulewicz, P., Fabian, M.P., 2018. Temporal trends in air pollution exposure inequality in Massachusetts. *Environ. Res.* 161, 76–86. <https://doi.org/10.1016/j.envres.2017.10.028>.
- Sacks, J.D., Lloyd, J.M., Zhu, Y., Anderton, J., Jang, C.J., Hubbell, B., Fann, N., 2018. The Environmental Benefits Mapping and Analysis Program – Community Edition (BenMAP-CE): a tool to estimate the health and economic benefits of reducing air pollution. *Environ. Model. Software* 104, 118–129. <https://doi.org/10.1016/J.ENVSOFT.2018.02.009>.
- Sperling, D., Eggert, A., 2014. California's climate and energy policy for transportation. *Energy Strategy Rev.* 5, 88–94. <https://doi.org/10.1016/J.ESR.2014.10.001>.
- Stoos, Christopher, 2021. Renewable Diesel Fuel Effects on Exhaust Emissions from a TIER 3 GE ES44C4 Locomotive.
- Tessum, C.W., Hill, J.D., Marshall, J.D., 2014. Life cycle air quality impacts of conventional and alternative light-duty transportation in the United States. *Proc. Natl. Acad. Sci. U.S.A.* 111 (52), 18490–18495. [https://doi.org/10.1073/PNAS.1406853111/SUPPL\\_FILE/PNAS.1406853111.SD01.XLS](https://doi.org/10.1073/PNAS.1406853111/SUPPL_FILE/PNAS.1406853111.SD01.XLS).
- Tessum, C.W., Paoletta, D.A., Chambliss, S.E., Apte, J.S., Hill, J.D., Marshall, J.D., 2021. PM2.5 polluters disproportionately and systemically affect people of color in the United States. *Sci. Adv.* 7 (18), 4491–4519. <https://doi.org/10.1126/sciadv.abf4491>.
- Thakrar, S.K., Balasubramanian, S., Adams, P.J., Azevedo, M.L., Muller, N.Z., Pandis, S. N., Polasky, S., Arden, C., Robinson, A.L., Apte, J.S., Tessum, C.W., Marshall, J.D., Hill, J.D., 2020. Reducing mortality from air pollution in the United States by targeting specific emission sources. *Cite This: Environ. Sci. Technol. Lett.* 7, 639–645. <https://doi.org/10.1021/acs.estlett.0c00424>.
- Thind, M.P.S., Tessum, C.W., Azevedo, I.L., Marshall, J.D., 2019. Fine particulate air pollution from electricity generation in the US: health impacts by race, income, and geography. *Environ. Sci. Technol.* 53 (23), 14010–14019. <https://doi.org/10.1021/ACS.EST.9B02527>.
- Tran, T., Tran, H., Mansfield, M., Lyman, S., Crosman, E., 2018. Four dimensional data assimilation (FDDA) impacts on WRF performance in simulating inversion layer structure and distributions of CMAQ-simulated winter ozone concentrations in Uintah Basin. *Atmos. Environ.* 177, 75–92. <https://doi.org/10.1016/J.ATMOSENV.2018.01.012>.
- United States Census Bureau, 2020. American Community Survey (ACS) Data. [https://www2.census.gov/geo/tiger/TIGER\\_DP/](https://www2.census.gov/geo/tiger/TIGER_DP/).
- US EPA, 2020. 2017 National Emissions Inventory Events and Nonroad Release and Updated Point Release.
- US EPA, 2021. Motor Vehicle Emission Simulator (MOVES3). <https://www.epa.gov/moves/latest-version-motor-vehicle-emission-simulator-moves>.
- Venecek, M.A., Yu, X., Kleeman, M.J., 2019. Predicted ultrafine particulate matter source contribution across the continental United States during summertime air pollution events. *Atmos. Chem. Phys.* 19 (14), 9399–9412. <https://doi.org/10.5194/ACP-19-9399-2019>.
- Wang, G., Bai, S., Ogden, J.M., 2009. Identifying contributions of on-road motor vehicles to urban air pollution using travel demand model data. *Transport. Res. Transport Environ.* 14 (3), 168–179. <https://doi.org/10.1016/j.trd.2008.11.011>.
- Wang, G., Jiang, R., Zhao, Z., Song, W., 2013. Effects of ozone and fine particulate matter (PM2.5) on rat system inflammation and cardiac function. *Toxicol. Lett.* 217 (1), 23–33. <https://doi.org/10.1016/j.toxlet.2012.11.009>.
- Werf van der, G.R., Randerson, J.T., Giglio, L., Leeuwen van, T.T., Chen, Y., Rogers, B.M., Mu, M., Marle van, M.J.E., Morton, D.C., Collatz, G.J., Yokelson, R.J., Kasibhatla, P. S., 2017. Global fire emissions estimates during 1997–2016. *Earth Syst. Sci. Data* 9, 697–720. <https://doi.org/10.5194/essd-9-697-2017>.
- Winkler, S.L., Anderson, J.E., Garza, L., Ruona, W.C., Vogt, R., Wallington, T.J., 2018. Vehicle criteria pollutant (PM, NOx, CO, HCs) emissions: how low should we go? *Npj Climate and Atmospheric Science* 2018 1 (1), 1–5. <https://doi.org/10.1038/s41612-018-0037-5>.
- World Bank, 2016. The Cost of Air Pollution. *The Cost of Air Pollution*. <https://doi.org/10.1596/25013>.
- World Health Organization, 2021. Fact Sheets: Ambient (Outdoor) Air Pollution. [https://www.who.int/news-room/fact-sheets/detail/ambient-\(outdoor\)-air-quality-and-health](https://www.who.int/news-room/fact-sheets/detail/ambient-(outdoor)-air-quality-and-health).
- Xing, Y.F., Xu, Y.H., Shi, M.H., Lian, Y.X., 2016. The impact of PM2.5 on the human respiratory system. *J. Thorac. Dis.* 8 (1), E69. <https://doi.org/10.3978/J.ISSN.2072-1439.2016.01.19>.
- Ying, Q., Fraser, M.P., Griffin, R.J., Chen, J., Kleeman, M.J., 2007. Verification of a Source-Oriented Externally Mixed Air Quality Model during a Severe Photochemical Smog Episode, vol. 41. *Atmospheric Environment*.
- Yu, X., Venecek, M., Kumar, A., Hu, J., Tanrikulu, S., Soon, S.T., Tran, C., Fairley, D., Kleeman, M.J., 2019. Regional sources of airborne ultrafine particle number and mass concentrations in California. *Atmos. Chem. Phys.* 19 (23), 14677–14702. <https://doi.org/10.5194/ACP-19-14677-2019>.
- Zhu, H., McCaffery, C., Yang, J., Li, C., Karavalakis, G., Johnson, K.C., Durbin, T.D., 2020. Characterizing emission rates of regulated and unregulated pollutants from two ultra-low NOx CNG heavy-duty vehicles. *Fuel* 277, 118192. <https://doi.org/10.1016/J.FUEL.2020.118192>.